Electron-hole Pair Dynamics and Strong Mott Pseudogap Effect in the Phase Diagram of Cuprates

M.Z. Hasan,[1, 2] Y. Li,[1] D. Qian,[1] Y.-D. Chuang,[3] H. Eisaki,[4] S. Uchida,[5] Y. Kaga,[6] T. Sasagawa,[6] and H. Takagi[4, 6]

[1]Department of Physics, Joseph Henry Laboratories, Princeton University, Princeton, NJ 08544
[2]CMC-CAT, Advanced Photon Source, Argonne National Laboratory, Argonne, IL 08544
[3]Advanced Light Source, Lawrence Berkeley National Lab, Berkeley, Ca 94720
[4]AIST, 1-1-1 Central 2, Umezono, Tsukuba, Ibaraki, 305-8568 Japan
[5]Department of Physics, University of Tokyo, Tokyo 113-8656, Japan
[6]Department of Adv. Materials Science, University of Tokyo, Kashiwanoha, Chiba 277-8561, Japan and CREST-JST, Kawaguchi, Saitama 332-0012, Japan

Introduction

The discovery of high temperature superconductivity, colossal magnetoresistance and other unusual electron transport behavior has led to extensive research interests in doped Mott insulators[1]-[7]. A parent Mott insulator can be doped either with electrons or holes, and many physical properties such as transport and magnetism are very sensitive to the doping level. Understanding the doping evolution of the electronic structure in both dopant-sides is therefore of crucial important in revealing the underling physics of the doped Mott system. High resolution resonant inelastic x-ray scattering (RIXS)[8, 9] is a recently developed powerful technique in investigating the Mott gap structure by resolving the particle-hole pair excitations along the momentum axis. Using the RIXS technique, we measured the doping evolution of the momentum dependent charge excitations over Mott gap in electron doped and hole doped cuprates.

Methods and Materials

We performed resonant inelastic x-ray scattering measurement on $Nd_{2-x}Ce_xCuO_4$ and $La_{2-x}Sr_xCuO_4$ single crystals by using the high resolution RIXS facilities at the CMC-CAT beamline 9-ID and BESSRC-CAT beamline 12-ID at the Advanced Photon Source, Argonne National Laboratory. The facilities are typical triple-axis spectrometers. The monochromatic incident energy was selected near Cu K edge to produce enhancement of the inelastic signals. The incident energy was then fixed and the scattered photon energy was scanned by Braggly reflecting the scattered photons from a germanium (733) crystal analyser. Finally the reflected photons were collected by a solid-state detector located at the focus of the analyser. The overall energy resolution was 370 meV and all the data were taken at room temperature. The momentum transfer varies by changing the scattering angle and the measurement was performed along [100] direction. The energy loss and the momentum transfer during the inelastic scattering measures the energy and the momentum of the excitations over the Mott gap. Eventually the dispersion relations of the excitations were mapped out.

Results

Fig.1 (top) shows pseudo-color plots of momentum-resolved charge excitation spectra in the electron-doped cuprate series $Nd_{2-x}Ce_xCuO_4$ (e-doped, x=0.10, 0.13) (a), hole doped cuprate series $La_{2-x}Sr_xCuO_4$ (h-doped, x=0.02, 0.14) (b) and undoped cuprate (x=0) (c) as a function of hole and electron doping (x) level. Quasielastic scattering was removed by fitting below 0.8 eV. A broad excitation band (cyan) is seen from 0.5 to 3 eV for the e-doped systems whereas the analogous excitations in the h-doped systems (red) appear in 2 to 5 eV energy range. These excitations are seen over the range of momentum transfers covering almost the full Brillouin zone. Fig.1(d) shows selected energy-loss spectra near high symmetry points of the Brillouin zone to compare the effect of hole and electron doping by comparing insulator vs. metal. The lower energy edge (dotted lines in Fig.1(top)) of the dominant excitation defines the edge of the insulating charge gap (effective Mott gap)

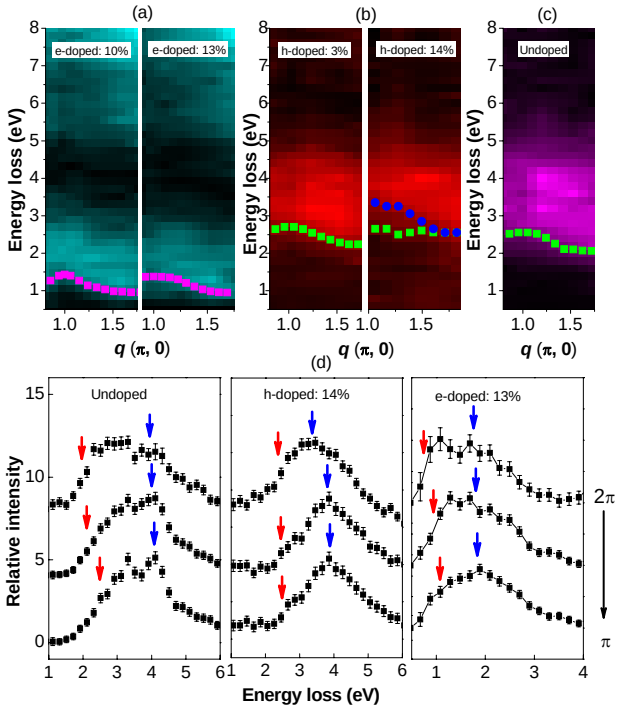

Fig. 1: Momentum-Resolved Charge Excitations in Cuprates: Momentum-dependence of charge excitations in electron-doped $Nd_{2-x}Ce_xCuO_4$ (a), hole-doped $La_{2-x}Sr_xCuO_4$ (b) and undoped insulator (c) copper oxides. Brighter color indicates higher intensity. Dotted lines indicate the location of the leading edge of the gap except in case of LSCO(x=0.14) where a second dotted line traces out the second peak. (d) shows selected energy-loss curves near high symmetry points of the Brillouin zone for undoped, h-doped, and e-doped samples

The excitation in undoped insulator shows a double peak feature within the whole Brillouin zone. With increased doping the spectra change in two major ways - a low-energy continuum appears below the gap as seen in Fig.2 and the momentum dependence of the leading edge weakens. A closer look in Fig.2

shows that the low-energy spectral weight grows (reddish/bluish continuum in Fig.1a and Fig.1b) at the expense of the spectral weight around 2 to 3.5 eV range in the insulator for hole doping and around 1 to 2 eV range for electron doping (Fig.2). This is clear evidence that even if doping introduces states in the middle of the gap (as argued based on ARPES measurements[10, 11]), changes in the electronic structure are further accompanied by direct melting (clear systematic changes in the leading-edge behavior) of the Mott gap in a momentum dependent manner. The observed low-energy continuum in the doped system is due to pair excitations involving quasiparticle-quasihole states that appear in the middle of the gap upon doping.

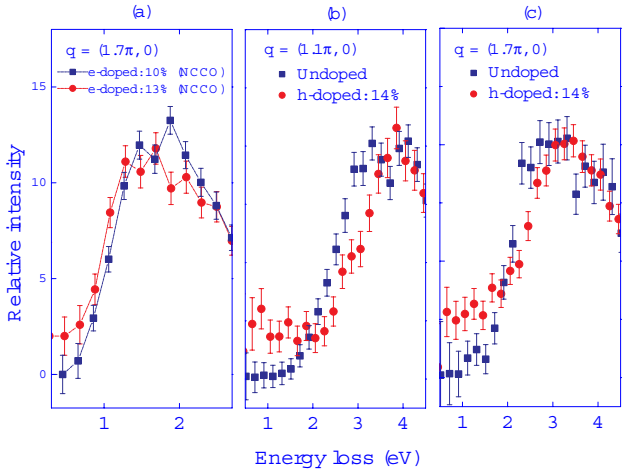

FIG. 2: Doping dependence of low-energy spectral weight with momenta near zone boundary for electron doping (left) and near zone center (middle) and near zone boundary (right) for hole doping.

Fig.3(left) shows the energy vs. momentum behavior of the excitations edges for both e-doped and h-doped systems. We determine the leading-edge mid-point by taking a derivative of the energy-loss spectra with respect to the energy-loss axis. Undoped insulator shows the largest amount of dispersion which is about 500 meV. Upon hole doping dispersion seems to flatten out in a systematic manner. For the 3% h-doping (insulator) dispersion is reduced and follows a qualitative trend as seen in the undoped insulator. In the 14% h-doped sample

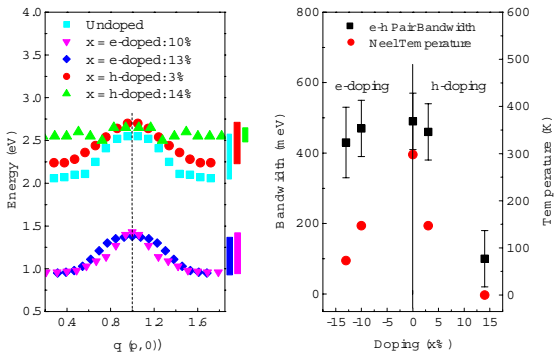

Fig. 3: (left) Energy vs. momentum relation of the leading-edge of the Mott gap determined by taking first derivatives of the image plots in Fig.1. Vertical bars outside the panel give a measure of the bandwidth. (right) Doping dependence of electron-hole pair bandwidth and Neel temperature.

dispersion is much reduced - it has flattened out quite a bit and is on the order of 100-150 meV. On the other hand, on the electron doping side, compared with undoped insulator, the dispersion shows only a little bit decrease even with electron doping as high as 13%, showing the asymmetry of the nature of the excitations between electron doped and hole doped systems.

Discussion

Our results show that a gap feature similar to the undoped insulator exists at all doping and its dispersion is a remnant behavior from the insulator at all momenta as seen from Fig.1 and 2. We refer to this feature in the doped system as the Mott pseudogap or remnant Mott gap. A remnant Fermi surface-like behavior of single-particle spectral weight, n(k), is observed in the undoped Mott insulator in ARPES studies by integrating within an energy window to include the occupied band [12]. In inelastic x-ray spectrum both occupied and unoccupied bands contribute hence our observation of remnant Mott gap in the doped system with similar momentum dispersion as in the insulator is consistent with a remnant Fermi surface (momentum behavior) behavior.

Looking at the dispersions as show in Fig.3(a), one can see that dispersion of pair excitations is weak from the zone center to about the half-way (1.5π, 0) to the zone boundary. In comparison with lattice simulations this effect has been argued to be due to the fact that the lowest energy state of the upper Hubbard band is near (π, 0) as opposed to the momentum of (π/2, π/2) of the top-most state of the lower Hubbard band[13, 14, 15]. Under this scenario, the x-ray spectra in lightly doped NCCO should not be much different from the undoped insulator since in the electron doped system lowest-energy excited electrons are in the upper Hubbard band and have very similar momenta as in the undoped insulator whereas in LSCO the lowest energy excited electrons are still in the lower (Zhang-Rice) Hubbard band. In other words, in case of hole doping, upper Hubbard band is not involved in creating the low energy electron-hole pair excitations hence the pair dynamics involves states of very different characters.

We look for possible direct correlation of electron-hole pair bandwidth measured in x-ray scattering and the Neel temperature which is the energy scale for the on-set of long-range antiferromagnetic order in these systems. Fig.3(right) plots the pair bandwidth and Neel temperature as a function of doping. This correlation suggests that pair bandwidth decreases as long-range magnetic correlations decrease with doping. However, the collapse of bandwidth is much faster with hole doping than it is for electron doping. For the hole doping, pair bandwidth shows a direct scaling with Neel temperature which suggests a direct correlation with antiferromagnetic order in the hole doped systems. In case of electron doping bandwidth suppression with doping is weaker and weakly correlated with the doping fall-off of antiferromagnetic order. Robustness of strong short-range antiferromagnetic order is clearly seen in neutron scattering studies of highly doped NCCO systems[16]. These results suggest that coherent propagation of electron-hole pairs are largely affected by the effective magnetic coupling or interaction strengths and reflects a strong electron-hole doping asymmetry in the electron dynamics of cuprates.

Our results reveal momentum structure of remnant Mott gap and electron-hole pair excitations in doped cuprates and their correlation with the phase diagram for the first time (Fig. 3 (right)). Although much theoretical efforts are needed to understand these observations we report here, results by

themselves shed new light on the theories that argue for an intimate connection between the pseudogap and Mott charge gap and the importance of magnetic coupling strength in describing correlated electron behavior in cuprates[3, 17].

We acknowledge M. Beno, D. Casa and T. Gog for technical help. The experiments were performed at BESSRC-CAT beamline 11-ID and CMC-CAT beamline 9-ID. Use of the Advanced Photon Source was supported by the U.S. Department of Energy, Office of Science, Office of Basic Energy Sciences, under Contract No. W-31-109-ENG-38. This work was partially supported by an NSF (DMR-0213706) grant. MZH acknowledges partial support through R.H. Dicke research award.

Reference

[1] N. F. Mott, Proc. Phys. Soc. London **A 62**, 416 (1949).
[2] J. Hubbard, Proc. Roy. Soc. London **A 277**, 237 (1964).
[3] P. W. Anderson, Science **235**, 1196 (1987).
[4] Y. Tokura, Physics Today **56(7)**, 50 (2003).
[5] V. J. Emery, S. A. Kivelson, Nature **374**, 434 (1995).
[6] M. Imada et.al., Rev. Mod. Phys. **70**, 1039 (1998).
[7] J. Orenstein, A. J. Millis, Science **288**, 468 (2000).
[8] P. M. Platzman, E. Isaacs Phys. Rev. **B 57**, 11107 (1998).
[9] C. C. Kao et al., Phys. Rev. **B 54**, 16361 (1996).
[10] A. Ino et.al., Phys. Rev. **B 62**, 4137 (2000).
[11] N.P. Armitage et.al., Phys. Rev. Lett. **87**, 147003 (2001).
[12] F. Ronning et.al., Science **282**, 2067 (1998).
[13] M. Z. Hasan et.al., Science **288**, 1811 (2000).
[14] K. Tsutsui, T. Tohyama and S. Maekawa Phys. Rev. Lett. **91**, 117001 (2003).
[15] K. Tsutsui, T. Tohyama and S. Maekawa Phys. Rev. Lett. **83**, 3705 (1999).
[16] K. Yamada et.al., Phys. Rev. Lett. **90**, 137004 (2003).
[17] R.B. Laughlin, Phys. Rev. Lett. **79**, 1726 (1997).